$T^-B^+NK^+$ severe combined immunodeficiency caused by complete deficiency of the CD3ζ subunit of the T-cell antigen receptor complex

Joseph L. Roberts,[1] Jens Peter H. Lauritsen,[2] Myriah Cooney,[1] Roberta E. Parrott,[1] Elisa O. Sajaroff,[1] Chan M. Win,[3] Michael D. Keller,[1] Jeffery H. Carpenter,[1] Juan Carabana,[3] Michael S. Krangel,[3] Marcella Sarzotti,[3] Xiao-Ping Zhong,[1,3] David L. Wiest,[2] and Rebecca H. Buckley[1,3]

[1]Department of Pediatrics and Immunology, Duke University Medical Center, Durham, NC; [2]Fox Chase Cancer Center, Division of Basic Sciences, Immunobiology Working Group, Philadelphia, PA; [3]Department of Immunology, Duke University Medical Center, Durham, NC

CD3ζ is a subunit of the T-cell antigen receptor (TCR) complex required for its assembly and surface expression that also plays an important role in TCR-mediated signal transduction. We report here a patient with $T^-B^+NK^+$ severe combined immunodeficiency (SCID) who was homozygous for a single C insertion following nucleotide 411 in exon 7 of the CD3ζ gene. The few T cells present contained no detectable CD3ζ protein, expressed low levels of cell surface CD3ε, and were nonfunctional. $CD4^+CD8^-CD3\varepsilon^{low}$, $CD4^-CD8^+CD3\varepsilon^{low}$, and $CD4^-CD8^-CD3\varepsilon^{low}$ cells were detected in the periphery, and the patient also exhibited an unusual population of $CD56^-CD16^+$ NK cells with diminished cytolytic activity. Additional studies demonstrated that retrovirally transduced patient mutant CD3ζ cDNA failed to rescue assembly of nascent complete TCR complexes or surface TCR expression in CD3ζ-deficient MA5.8 murine T-cell hybridoma cells. Nascent transduced mutant CD3ζ protein was also not detected in metabolically labeled MA5.8 cells, suggesting that it was unstable and rapidly degraded. Taken together, these findings provide the first demonstration that complete CD3ζ deficiency in humans can cause SCID by preventing normal TCR assembly and surface expression. (Blood. 2007; 109:3198-3206)

Introduction

Severe combined immunodeficiency (SCID) is a syndrome characterized by absent T- and B-lymphocyte function that is uniformly fatal in infancy without successful immune reconstitution.[1-3] Several different molecular etiologies of SCID in humans have been described. These include mutations in genes encoding components of lymphocyte cytokine receptors,[4-11] gene products responsible for T- and B-cell antigen receptor VDJ recombination,[12-17] proteins instrumental in lymphocyte survival[18] or function,[19,20] and structural subunits of the T-cell antigen receptor (TCR) complex.[21,22] The multimeric TCR complex is composed of a clonotypic TCRαβ or TCRγδ heterodimer associated with invariant CD3 (CD3γ, CD3δ, CD3ε, and CD3ζ) chains.[23-26] TCR complexes are assembled in the endoplasmic reticulum of mature T cells in stepwise fashion, with the final stage being association of CD3ζ homodimers with incomplete TCRαβ-CD3γ-CD3δ-CD3ε complexes.[27-35] The addition of CD3ζ subunits is critical for survival and efficient transport of TCR complexes to the plasma membrane,[31,34] as incomplete TCRαβ-CD3γ-CD3δ-CD3ε complexes are rapidly degraded in lysosomes.[34] TCR complex ligand-binding specificity is provided by the clonotypic TCRαβ or TCRγδ heterodimer,[36] whereas CD3 chains serve as signal transducing subunits via their cytoplasmic immunoreceptor tyrosine-based activation motifs (ITAMs).[37-40] CD3γ, CD3δ, and CD3ε chains each contain one ITAM; CD3ζ contains 3. Phosphorylation of CD3 chain ITAMs following TCR ligand engagement results in recruitment and activation of ZAP-70, a protein tyrosine kinase required for normal T-cell signaling.[41,42] Hence, surface TCR complex expression is required for both antigen recognition and signal transduction following ligand binding in mature T cells. TCR expression is also vital for T-cell development in the thymus[43-46] and murine gene knockout studies have demonstrated the importance of individual components of the TCR complex in this process. Mice lacking expression of TCRβ,[47] CD3γ,[48] or CD3ε[49] exhibited a block at the $CD4^-CD8^-$ stage of thymocyte development, whereas $CD4^+CD8^+$ cells accumulated in TCRα-deficient[47,50] or CD3δ-deficient animals.[51] Development of $CD4^+CD8^+$ thymocytes, $CD4^+$ and $CD8^+$ single-positive thymocytes, and peripheral T cells was markedly diminished in mice lacking CD3ζ.[52-55] Abnormalities in expression of CD3 subunits of the TCR complex have also been reported in humans. Absence of CD3δ expression led to SCID with a block in T-cell ontogeny prior to the $CD4^+CD8^+$ stage of thymocyte development.[21,22] A homozygous CD3ε gene mutation expected to prevent protein expression has been described in a SCID patient.[22] Partial CD3ε deficiency[56,57] and complete CD3γ deficiency[58,59] did not completely block T-cell development and resulted in milder immunodeficiency. A complex case of CD3ζ deficiency partially corrected by somatic mutations has recently been reported in a patient with recurrent infections and decreased numbers of peripheral T cells.[60] In the present study we describe a unique infant with $T^-B^+NK^+$ SCID due to complete CD3ζ deficiency.

Submitted August 25, 2006; accepted December 5, 2006. Prepublished online as *Blood* First Edition Paper, December 14, 2006; DOI 10.1182/blood-2006-08-043166.

The publication costs of this article were defrayed in part by page charge payment. Therefore, and solely to indicate this fact, this article is hereby marked "advertisement" in accordance with 18 USC section 1734.

Patient, materials, and methods

Patient

The patient was the child of unrelated parents of Chamorro descent from Guam. She presented with pneumonia of unknown etiology at 4 months of age and subsequently developed a chronic cough, recurrent otitis media, failure to thrive, a chronic mild rash, and one episode of *Salmonella* gastroenteritis. At age 10 months she was hospitalized for thrombocytopenia and found to have a cytomegalovirus (CMV) infection. Initial immune studies in Guam and Hawaii revealed very low numbers of circulating T cells (141/mm^3) and absent T-cell proliferative responses. The patient was referred to Duke University Medical Center where the diagnosis of SCID was confirmed, treatment of her CMV infection was begun, and, at age 12 months, she received a T cell-depleted haploidentical bone marrow transplant from her mother without pretransplantation chemotherapeutic conditioning or posttransplantation graft-versus-host disease (GVHD) prophylaxis. She received a low number of cells with this transplant and showed no evidence of immune function over the next 4 months so received a second T cell-depleted maternal marrow transplant without preconditioning or GVHD prophylaxis at 16 months of life. The patient continued to show no signs of T-cell chimerism or function after her second transplant perhaps due, at least in part, to ongoing CMV viremia. She received a third stem cell transplant from her father without preconditioning or GVHD prophylaxis and remains clinically stable at 1 month after transplantation.

Immunologic phenotype analysis

Standard 4-color flow cytometry of peripheral blood lymphocytes was performed with labeled antibodies (Abs) to CD3ε (clone SK7 or clone UCHT1), CD4, CD8, CD14, CD16, CD20, CD45, CD56 (clone NCAM16.2), TCRαβ (clone T10B9.1A-31), TCRγδ (clone B1), and HLA-A2 (clone BB7.2) purchased from BD Biosciences (San Jose, CA). A second anti-CD56 Ab (clone MEM188) (eBioscience, San Diego, CA) was used in some experiments. CD3ε^{high} and CD3ε^{low} cell numbers in Table 1 were calculated from anti-CD3ε staining data shown in Figure 1 using the depicted gates to define the number of (CD3ε^{high} cells plus CD3ε^{low} cells), and additional gates (fluorescence intensity $\geq 10^2$ for anti-CD3ε-APC staining, and $\geq 5 \times 10^1$ for PerCP-labeled anti-CD3ε staining) to quantify CD3ε^{high} cells. Anti-CD3ζ (clone 6B10.2; Santa Cruz Biotechnology, Santa Cruz, CA) recognizing amino acids 36-54 of the molecule was used for flow cytometric detection of CD3ζ in fixed and permeabilized cells as described.[11] Spectratype analysis of TCR Vβ repertoire by reverse transcription-polymerase chain reaction (RT-PCR)[61] and real-time PCR analysis of signal joint TCRδ excision circles (TRECs)[62] were performed as described.[63,64] Serum immunoglobulin levels were determined by nephelometry. Lymphocyte proliferation was assessed by measuring [^{3}H]thymidine incorporation into mononuclear cells following culture with optimal concentrations of the indicated stimuli as described.[65] Natural killer (NK) cell function was measured as percent specific lysis of ^{51}Cr-labeled K562 targets by peripheral blood mononuclear cells (PBMCs) at the indicated effector-to-target (E/T) ratios. All studies were performed with the approval of the Duke University Health System's Institutional Review Board for Clinical Investigations, and written informed consent in accordance with the Declaration of Helsinki was obtained from the patient's parents.

Table 1. Patient immunologic phenotype

	Patient	Controls
Lymphocyte subpopulation*		
CD3ε^{high}	17 (0.4)	1111-5183
CD3ε^{low}	2688 (63.7)	NA
CD20$^+$	1401 (33.2)	144-671
CD16$^+$	174 (4.1)	152-709
CD56$^+$	0	223-1040
Serum Ig level†		
IgG‡	2310	192-515
IgA	213	12-31
IgM	248	39-92
IgE	27	0-150
Proliferative stimulus§		
Medium	1254	693 ± 825
PHA	1989	222 330 ± 50 643
Con A	3695	208 534 ± 52 592
PWM	7224	135 520 ± 35 077
Candida	1000	45 431 ± 30 989
Anti-CD3ε	131	122 953 ± 44 094
Autologous cells	745	3163 ± 2874
Allogeneic cells	5520	59 818 ± 38 445

NA indicates not applicable; PHA, phytohemagglutinin; Con A, concanavalin A; PWM, pokeweed mitogen.

*Values are expressed as cells/mm^3 or (percentage of lymphocytes). Control values are the 95% confidence intervals for 1550 healthy controls.

†Values are expressed as mg/dL (IgG, IgA, IgM) or U/mL (IgE). Normal values are the 95% confidence intervals for 12 6-month-old control subjects.

‡The patient was receiving IVIG when the IgG level was measured.

§Values are cpm [^{3}H]thymidine incorporation. Controls values are the mean ± SD of responses in 167 healthy controls.

Cell sorting

Patient and healthy volunteer CD3ε$^+$ cells used for real-time PCR and immunoblotting were isolated from PBMCs using a fluorescence-activated cell sorting (FACS) Vantage SE (Becton Dickinson, San Jose, CA) by sorting cells stained brighter with anti-CD3ε (clone SK7; BD Biosciences) than with isotype control Ab. Patient PBMCs used for sorting were shown to be free of detectable maternal cells by staining with antibody to HLA-A2 (BD Biosciences), an unshared maternal histocompatibility antigen.

Real-time quantitative PCR analysis of CD3ζ mRNA expression

RNA isolated from sorted CD3ε$^+$ cells (RNeasy Mini Kit; Qiagen, Santa Clarita, CA) was used for cDNA synthesis (SuperScript II Preamplification System; Invitrogen, Carlsbad, CA). CD3ζ and β-actin transcripts were then quantified by real-time PCR with a Roche LightCycler and FastStart DNA Master SYBR Green I Kit (Roche Diagnostics, Indianapolis, IN). The CD3ζ primers (5′-CAGCCTCTTTCTGAGGGAAA and 5′-AGGATTCCATCCAGCAGGTA) used for amplification were upstream of both the patient exon 7 mutation site and the region altered in transcript variant 1. CD3ζ transcript levels were normalized to those for β-actin in each sample.

CD3ζ sequence analysis

gDNA templates isolated from whole blood (DNeasy Tissue Kit; Qiagen) were PCR-amplified with primer pairs (sequences available on request) spanning each of the 8 CD3ζ exons and surrounding intron splice sites. PCR products were purified (Qiaex II Gel Extraction Kit; Qiagen) and used as templates in sequencing reactions (Big Dye Terminator Cycle Sequencing System; Perkin Elmer Life Sciences, Boston, MA). Sequencing reactions representing both strands were analyzed using an ABI 377 Prism DNA (Perkin Elmer) instrument and software. The detected 411insC mutation was further evaluated by sequence analysis of gDNA obtained from the patient's parents and 50 unrelated healthy individuals of varied ethnic backgrounds (Alzheimer's Disease Research Center, Duke University Medical Center, Durham, NC). Nucleotide numbers refer to the published cDNA sequence of canonical CD3ζ transcript variant 2 (NM000734)[66] with start codon = 1.

Molecular modeling

Patient mutant CD3ζ protein sequence analysis and structure prediction were performed by the Molecular Modeling Facility, Fox Chase Cancer Center (Philadelphia, PA). In these studies, wild-type and D138fsX272 mutant CD3ζ sequences were used to perform a multiple-round sequence search using the position-specific iterated basic alignment search tool (PSI-BLAST)[67] against the National Center for Biotechnology Information (NCBI) nonredundant sequence database. The profiles obtained after each round were used to generate the secondary structure prediction, using

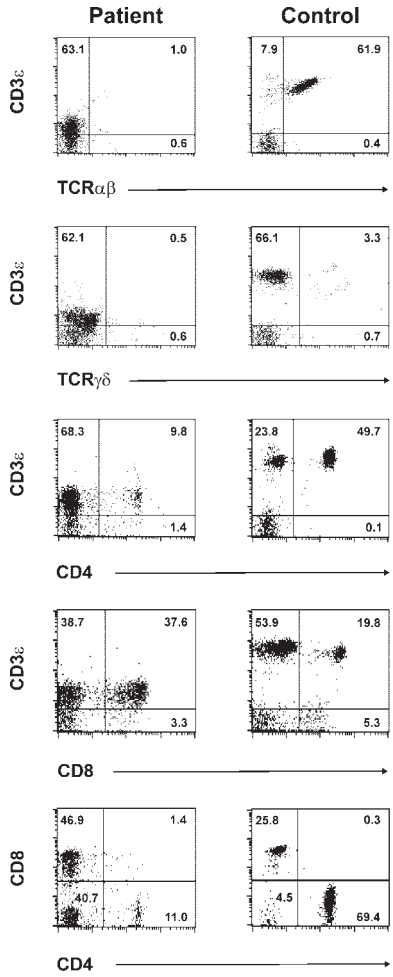

Figure 1. Phenotype of patient CD3ε$^+$ cells. Patient and healthy volunteer PBMCs were stained and analyzed by 4-color flow cytometry. Data were collected on CD14$^-$CD45$^+$ lymphocytes. Shown are 2-color plots of cells stained with PerCP-labeled anti-CD3ε plus anti-TCRαβ-FITC (top row 1), PerCP-labeled anti-CD3ε plus anti-TCRγδ-PE (row 2), anti-CD3ε-APC and anti-CD4-FITC (row 3), or anti-CD3ε-APC and anti-CD8-PerCP (row 4). The 2-color plots in bottom row 5 depict anti-CD4-FITC and anti-CD8-PerCP staining on software-gated CD3ε$^+$ cells. The selected gate is shown in rows 3 and 4 and was based on anti-CD3ε-APC staining intensity. Numbers represent the frequency of cells present in the indicated quadrant.

protein secondary structure prediction program (PSIPRED)[68] for computation and molecular integrated development environment (MolIDE)[69] for graphical rendering. Next, the Protein Data Bank (PDB)[70] was searched for the availability of proteins with known structures that could be used as templates for homology modeling. Transmembrane hidden Markov model (TMHMM)[71] Server (Center for Biological Sequence Analysis, Technical University of Denmark, Lyngby, Denmark) was used to predict transmembrane regions in both the wild-type and mutant sequences. A customized high-sensitivity sequence search (e value = 500, effective length of the database = 100) was performed against the nonredundant sequence database using missense residues of the mutant CD3ζ. A sequence motif (MOTIF) Search (GenomeNet, Bioinformatics Center, Institute for Chemical Research, Kyoto University, Kyoto, Japan) was also performed for this region of patient mutant CD3ζ.

Plasmids, mutagenesis, and transfection

Full-length cDNA encoding wild-type CD3ζ transcript variant 2 (NM000734),[66] designated hsCD3ζWT, was PCR-amplified from a human cDNA library using CD3ζ primers (5′-CGGAAT TCCCTCCCAGCCTCTT-TCTGAG and 5′-TCCGCTCGAGCTAGCATCTGCGCTTTCTCT) and directionally cloned into pBluescript (Stratagene, La Jolla, CA). The patient cytosine insertion mutation (hsCD3ζCm) was created by site-directed mutagenesis. Variant constructs hlCD3ζWT and hlCD3ζCm containing the longer CD3ζ splice variant 1 (NM198053)[66] that includes an additional codon encoding amino acid Q101 due to use of an alternate 5′ splice site in intron 4[72-74] were similarly generated using 2 hCD3ζ internal primers (CD3ζ424R: 5′ CGGCTTTCCCCCCATCTCA, and CD3ζ425F: 5′ CA-GAGAAGGAAGAACCCTCAGGA). Cloning details will be provided on request. After sequence verification, wild-type and mutant constructs were subcloned into a modified version of p-MSCV-IRES-eGFP (pMiG)[75,76] with an expanded multiple cloning site (Dario Vignali, St Jude Children's Research Hospital, Memphis, TN). Phoenix-E retroviral packaging cells were transfected with retroviral vectors using the calcium phosphate transfection method as described.[77] Transfection efficiencies were evaluated by determining the percentage of eGFP$^+$ Phoenix-E cells using flow cytometry (FACSvantage SE; Becton Dickinson). The CD3ζ-deficient murine T hybridoma, MA5.8,[34] was then transduced with retroviral supernatant treated with 8 μg/mL Polybrene.

Flow cytometry analysis of retrovirally transduced MA5.8 cells

Retrovirally transduced cells were isolated by flow cytometry based on eGFP expression as described.[78] Alternatively, mixed populations were stained with anti-TCRβ Ab (clone H57-597)[79] or anti-CD3ε Ab (clone 145-2C11)[80] following which the effect of the transduced construct on TCR expression was evaluated on electronically gated eGFP$^+$ cells using Flowjo software (Treestar, Ashland, OR).

Immunoprecipitation and immunoblotting

Sorted CD3ε$^+$ PBMCs or retrovirally transduced MA5.8 cells were lysed in digitonin (EMD Biosciences, San Diego, CA) lysis buffer (1% digitonin, 50 mM Tris pH 7.4, 150 mM NaCl, 1 mM Na_2VO_4, 2 mM EDTA), and a complete protease inhibitor cocktail (Roche, Basel, Switzerland). Lysates from 8×10^5 CD3ε$^+$ cells were sequentially immunoprecipitated with 2 rounds of anti-CD3ε (clone 145-2C11) followed by anti-CD3ζ Ab (clone 6B10.2; Santa Cruz Biotechnology) as described,[81] whereas lysates from the remaining 2×10^5 CD3ε$^+$ cells were subjected to direct immunoblotting. CD3ε$^+$ and MA5.8 cell lysates were then resolved by 13% sodium dodecyl sulfate-polyacrylamide gel electrophoresis (SDS-PAGE) and blotted with Ab to CD3ε (clone HMT3)[82] and CD3ζ (clone 6B10.2; Santa Cruz Biotechnology) as described.[83] Membranes containing transferred MA5.8 lysates were also probed with anti-Calnexin Ab (David McKean, Mayo Clinic, Rochester, MN).[84]

Metabolic labeling

MA5.8 cells[34] were labeled in cysteine- and methionine-free medium containing [^{35}S]methionine for 30 minutes, following which digitonin extracts were either sequentially immunoprecipitated with anti-CD3ε (clone 145-2C11) followed by anti-CD3ζ Ab (clone 6B10.2; Santa Cruz Biotechnology), or immunoprecipitated with anti-CD3ζ Ab alone as described.[81] Isolated TCR subunits were resolved by SDS-PAGE and visualized by fluorography.

Results

Patient immunologic phenotype

Evaluation of patient peripheral blood lymphocytes by flow cytometry at age 11 months revealed markedly diminished numbers of normal mature T cells expressing high levels of surface CD3ε (CD3ε^{high}), with increased numbers of CD20-bearing B cells and normal numbers of CD16$^+$ NK cells (Table 1). Dual staining CD56$^+$ CD16$^+$ NK cells were not detected due to the absence of measurable surface CD56 expression on patient cells using 2 different anti-CD56 Abs (clone NCAM16.2, clone MEM188; Table 1). Of note, essentially all of the patient's T cells consistently

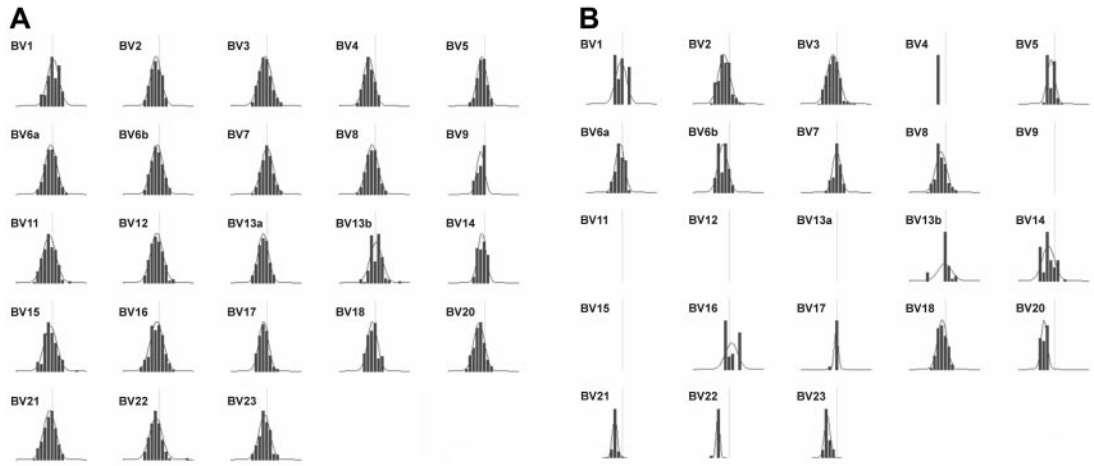

Figure 2. Spectratype analysis of patient TCR Vβ repertoire. Expression of the indicated Vβ families in (A) healthy volunteer and (B) patient cells was assessed by PCR amplification and run-off reaction. Depicted are density peak histograms for each Vβ family with CDR3 sizes centered around a CDR3 length = 30 bp (vertical line) shown on the x-axis, and peak fluorescence intensity on the y-axis. The calculated Kullback-Leibler divergence (DKL), a statistical measure of divergence from maximum diversity, was 0.05 for healthy volunteer histograms and 0.25 for patient histograms. The higher patient DKL indicates a less diverse (more oligoclonal) distribution of peaks.

expressed very low levels of surface CD3ε ($CD3\varepsilon^{low}$) compared with that of normal control cells (Figure 1; Table 1). Similar results were obtained following staining with either of 2 different anti-CD3ε Abs (clone SK7, clone UCHT1; data not shown). In addition, very few patient $CD3\varepsilon^{low}$ cells coexpressed detectable surface TCRαβ or TCRγδ (Figure 1) by flow cytometry. $CD4^+CD3\varepsilon^{low}$ and $CD8^+CD3\varepsilon^{low}$ patient cells were both present, with the $CD8^+$ population being more prevalent (Figure 1). Further analysis of CD4 and CD8 expression on software-gated peripheral blood $CD3\varepsilon^{low}$ cells (Figure 1 bottom panels) revealed a markedly increased frequency of $CD4^-CD8^-CD3\varepsilon^{low}$ cells in the patient (40.7%). Spectratype analysis of patient PBMCs revealed an oligoclonal Vβ repertoire similar to those previously noted in other SCID patients prior to immune reconstitution (Figure 2B).[63] Although not normal, these results nonetheless demonstrate that TCR Vβ genes had undergone productive rearrangements in patient T cells. TRECs were not detected in patient PBMCs (data not shown). Additional studies revealed that patient T-cell proliferative responses to mitogens, *Candida* antigen, anti-CD3ε Ab, and allogeneic cells were all profoundly depressed at presentation (Table 1), commensurate with a diagnosis of SCID. Serum IgA and IgM levels were elevated and IgE was present in normal amounts at this time. The patient had received intravenous immunoglobulin (IVIG) shortly before measurement of her serum IgG level. Despite the absence of surface CD56 expression, patient NK effector cells exhibited detectable, albeit low, lytic activity against labeled K562 targets (Figure 3). The diminished level of patient NK function noted in this experiment was not simply due to a lower frequency of patient effector cells because the number of patient and healthy volunteer $CD16^+$ cells present in the assay were similar.

Patient CD3ζ expression levels and mutation analysis

Because of the abnormalities in patient cell surface CD3ε expression noted, we next examined expression of CD3ε along with that of another CD3 chain, CD3ζ, in immunoblots of whole-cell lysates prepared from sorted $CD3\varepsilon^+$ cells. CD3ε protein levels were similar in patient $CD3\varepsilon^{low}$ (Figure 4A lane 7) and healthy control $CD3\varepsilon^{high}$ (Figure 4A lane 3) cells in this experiment. CD3ζ was also abundant in healthy control T cells but was not detected in the equivalent patient sample (Figure 4A lanes 3 and 7). Likewise, we were also unable to detect CD3ζ in permeablized patient PBMCs by flow cytometry (Figure 4B). Despite the absence of CD3ζ protein, real-time quantitative PCR revealed abundant levels of CD3ζ mRNA in sorted patient $CD3\varepsilon^{low}$ PBMCs (Figure 4C). Given the lack of detectable CD3ζ protein expression in patient $CD3\varepsilon^{low}$ cells, we performed CD3ζ sequence analysis and found the patient to be homozygous for a single C insertion in exon 7 following nucleotide 411 of the coding sequence (411insC). Sequencing of patient CD3γ, CD3δ, and CD3ε genes revealed them to be wild type. The patient's mother and father were both heterozygous for the 411insC CD3ζ mutation, and this sequence abnormality was not detected in gDNA from any of the 50 unrelated healthy individuals analyzed. The C insertion causes a frameshift commencing at amino acid 138 that disrupts expression of the third CD3ζ ITAM (beginning at G139)[40] and leads to termination at missense amino acid position 272 (D138fsX272), well beyond wild-type termination codon 164. Hence, unphosphorylated, monomeric, mutant D138fsX272 CD3ζ has a predicted molecular mass (29 kDa) greater than wild-type (16 kDa) CD3ζ (Figure 5). No sequence motifs or regions of homology with known proteins were detected in the mutant CD3ζ sequence and no structure could be confidently assigned to this region by molecular modeling analysis. There were 2 relatively hydrophobic stretches centered around missense amino acids 200 and 250 identified that may represent helices; however, the prediction probability for this was not very high (< 0.5). It is important to note that the epitope recognized by the anti-CD3ζ Ab

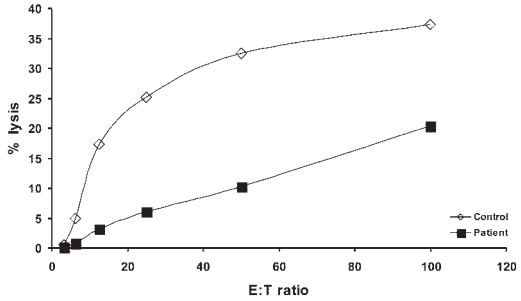

Figure 3. Patient NK cell function. Values represent the percent specific lysis of ^{51}Cr-labeled K562 target cells by patient or healthy control PBMCs, as indicated, following incubation for 4 hours at effector-to-target (E/T) ratios of 3:1, 6:1, 12:1, 25:1, 50:1 and 100:1.

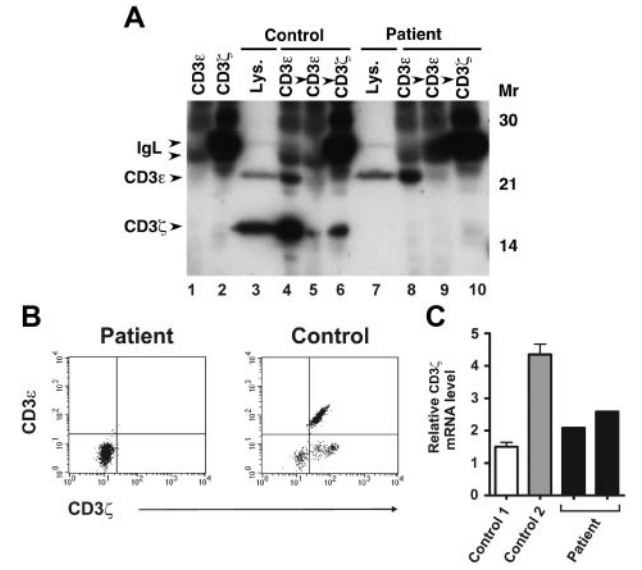

Figure 4. Analysis of CD3ζ protein and mRNA expression in patient T cells. (A) Patient and healthy volunteer sorted CD3ε^+ PBMCs were lysed in digitonin lysis buffer and either sequentially immunoprecipitated with 2 rounds of anti-CD3ε Ab followed by anti-CD3ζ Ab, or subjected to direct immunoblotting (lanes 3 and 7). Lysates were immunoblotted with anti-CD3ζ and anti-CD3ε Abs. Lanes 1 and 2 contain anti-CD3ε– or anti-CD3ζ–coated beads incubated with lysis buffer alone, as indicated. (B) Patient and healthy volunteer PBMCs were first stained with PerCP-labeled anti-CD3ε to assess cell surface CD3ε expression. The cells were then fixed and permeabilized, stained with FITC-labeled anti-CD3ζ Ab, and analyzed by flow cytometry. Shown are 2-color plots of surface CD3ε and intracellular CD3ζ expression. (C) Patient CD3ε^+ cells were obtained from 2 different sorted PBMC samples (from different dates). Healthy volunteer sorted CD3ε^+ PBMCs were isolated from 2 unrelated individuals (control 1, control 2). cDNA was prepared from sorted cells and CD3ζ transcripts were quantified by SYBR green real-time PCR. Levels of CD3ζ mRNA were normalized to those of β-actin for each sample. Values represent mean ± SEM of duplicate determinations.

used in our studies lies upstream (amino acids 36-54) of the mutation (Figure 5). Nevertheless, no 29-kDa species was detected in patient CD3ε^{low} cells (Figure 4A lane 7).

Patient mutant CD3ζ protein fails to support cell surface TCR expression due to rapid degradation

We next examined steady-state assembly of TCR complexes in patient T cells homozygous for the 411insC CD3ζ mutation. Association of CD3ζ homodimers with incomplete TCRαβ-CD3γ-CD3δ-CD3ε complexes is the final step in TCR assembly and is necessary for survival and efficient transport of complete TCR complexes from the endoplasmic reticulum to the cell surface.[27-35] In these experiments, lysates prepared from sorted CD3ε^{low} patient and CD3ε^{high} normal control PBMCs were sequentially immunoprecipitated with 2 rounds of anti-CD3ε Ab to isolate CD3ζ-containing complete TCR complexes, followed by anti-CD3ζ immunoprecipitation to capture any remaining, unassembled, CD3ζ.[81] Immunoblotting of the immunoprecipitated samples from normal control T cells revealed that substantial quantities of CD3ζ associated with CD3ε in complete TCR complexes (Figure 4A lane 4), with a smaller amount of free CD3ζ (Figure 4A lane 6) remaining in the anti-CD3ζ immunoprecipitate. This free CD3ζ did not result from failure to capture all of the complete TCR complexes because blotting with anti-CD3ε Ab revealed that all of the CD3ε was captured in the initial immunoprecipitate (Figure 4A; compare lanes 4 and 5). In marked contrast, no CD3ζ was detected in the patient samples, either at the 16-kDa size of wild-type CD3ζ or at the 29-kDa size predicted for the D138fsX272 mutant (Figure 4A lanes 7-10), despite the presence of immunoprecipitated CD3ε (Figure 4A lane 8).

The absence of detectable mutant CD3ζ protein in patient CD3ε^{low} cells in this experiment may have been due to (1) poor expression or rapid degradation of D138fsX272 mutant CD3ζ protein prior to assembly with other TCR chains, (2) impaired assembly of D138fsX272 mutant chains with incomplete TCRαβ-CD3γ-CD3δ-CD3ε complexes leading to a paucity of complete TCR complexes, or (3) inefficient transport of D138fsX272 mutant CD3ζ-containing complete TCR complexes to the plasma membrane. To distinguish among these possibilities, we analyzed TCR assembly and surface expression in MA5.8 cells transduced with patient 411insC mutant or wild-type human CD3ζ cDNA retroviral constructs. MA5.8 is a CD3ζ-deficient murine T-cell hybridoma[34] in which expression of human CD3ζ efficiently restores surface TCR expression.[85] For these studies, retroviral expression constructs containing the patient C insertion mutation in each of 2 prevalent human CD3ζ transcript variants[74] were generated by site-directed mutagenesis using PCR. The longer CD3ζ transcript variant 1 (NM198053)[66,72-74] uses an alternate 5′ splice site in intron 4 and encodes a longer CD3ζ protein isoform including amino acid Q101 that is not present in canonical transcript variant 2 (NM000734).[66] Assessment of transduced MA5.8 cells by flow cytometry revealed that expression of wild-type CD3ζ, but not patient mutant CD3ζ, cDNAs effectively restored cell surface TCR expression, as measured by TCRβ and CD3ε staining (Figure 6A). Immunoblot analysis of transduced MA5.8 cell lysates also demonstrated expression of transduced 16-kDa CD3ζ protein (Figure 6B upper panel, lanes 2 and 4) and stabilization of endogenous CD3ε expression (Figure 6B middle panel, lanes 2 and 4) by wild-type CD3ζ constructs. However, as was the case in patient CD3ε^{low} cells (Figure 4A), we were unable to detect expression of 29-kDa mutant CD3ζ protein in transduced MA5.8 cells (Figure 6B upper panel, lanes 3 and 5). Similarly, endogenous CD3ε protein was not stabilized in cells transduced with mutant CD3ζ constructs (Figure 6B, compare lanes 3 and 5 to lane 1).

To directly determine if nascent, D138fsX272 mutant CD3ζ subunits assemble properly with other TCR chains, MA5.8 cells

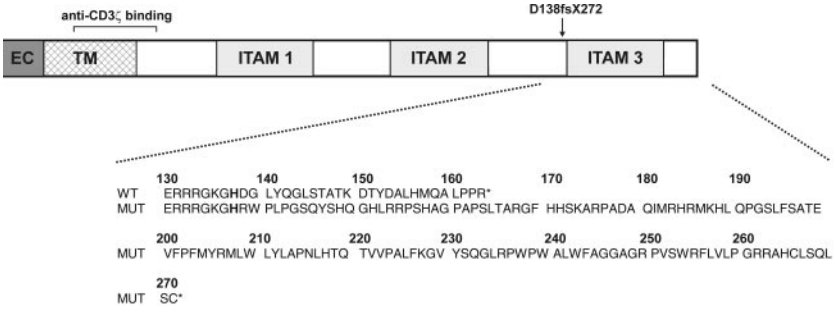

Figure 5. Diagram of patient CD3ζ mutation. The extracellular (EC), transmembrane (TM), and 3 intracellular ITAMs of wild-type CD3ζ protein are depicted along with the location of the homozygous patient mutation and the recognition site of the anti-CD3ζ Ab used in the present study. Wild-type (WT) and patient (MUT) CD3ζ amino acid sequences in the region affected by the mutation are shown in the expanded view. X indicates stop codon; and fs, frameshift.

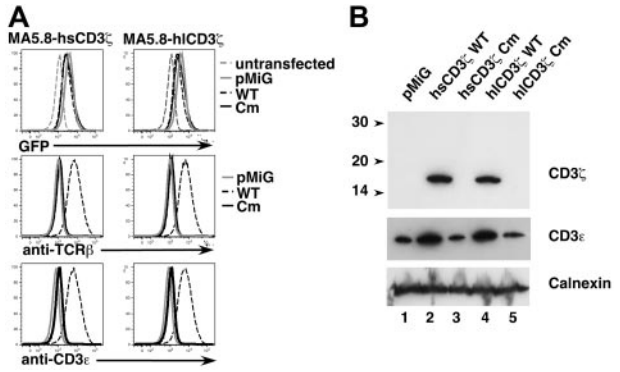

Figure 6. Patient mutant CD3ζ fails to rescue TCR expression in retrovirally-transduced CD3ζ-deficient MA5.8 cells. (A) MA5.8 cells were transduced with individual retroviral vectors containing one of the following human CD3ζ cDNAs: hsCD3ζWT (wild-type CD3ζ transcript variant 2), hsCD3ζCm (patient 411insC mutant CD3ζ transcript variant 2), hlCD3ζWT (wild-type CD3ζ transcript variant 1), or hlCD3ζCm (patient mutant CD3ζ transcript variant 1). Cells were also transduced with pMiG vector alone. Depicted are 1-color histograms of transduced MA5.8 cells analyzed for expression of eGFP indicator protein, surface TCRβ, or surface CD3ε by flow cytometry. (B) MA5.8 cells retrovirally transduced with the indicated cDNAs were lysed in digitonin lysis buffer, resolved by SDS-PAGE, and immunoblotted with anti-CD3ζ Ab (top panel) and anti-CD3ε Ab (middle panel). The membrane was also probed with anti-Calnexin Ab (bottom panel) to assess gel loading.

transduced with wild-type or 411insC mutant CD3ζ transcript variant 2 constructs were metabolically labeled for 30 minutes and analyzed by sequential immunoprecipitation with anti-CD3ε Ab to detect CD3ζ in complete TCR complexes, followed by anti-CD3ζ Ab to capture unassembled CD3ζ, or immunoprecipitation with anti-CD3ζ Ab alone. Only incomplete TCRαβ-CD3γ-CD3δ-CD3ε complexes lacking detectable CD3ζ were immunoprecipitated with anti-CD3ε Ab in MA5.8 cells transduced with vector alone (Figure 7 lane 7) as expected, and CD3ζ was not identified in these cells (Figure 7 lanes 7-9). Consistent with the rescue of cell surface TCR expression noted in this study (Figure 6A) and in a previous report,[85] newly synthesized CD3ζ assembled in complete TCR complexes was readily apparent in MA5.8 cells transduced with wild-type CD3ζ (Figure 7 lane 1). However, in cells transduced with the 411insC mutant CD3ζ, ectopically expressed CD3ζ was not detected in any form (Figure 7 lanes 4-6), thereby preventing the generation of complete TCR complexes (Figure 7 lane 4). Taken together, these data demonstrate that D138fsX272 mutant CD3ζ protein fails to assemble into complete TCR complexes and is likely to be rapidly degraded.

Discussion

This report describes an infant with $T^-B^+NK^+$ SCID due to a homozygous 411insC mutation in the gene encoding the CD3ζ subunit of the TCR complex. The defects in T-cell development and function noted in this patient are comparable to those previously described in mice lacking CD3ζ expression due to targeted gene disruption.[52-55] CD3ζ-deficient mice expressed normal numbers of immature $CD4^-CD8^-$ thymocytes but markedly diminished development of $CD4^+CD8^+$ thymocytes, and very low numbers of $CD4^+$ and $CD8^+$ single-positive TCRαβ thymocytes and peripheral T cells that expressed low levels of surface CD3ε and were nonfunctional.[52-55] Productive TCRβ gene rearrangements, which commence at the $CD4^-CD8^-CD44^{-/low}CD25^+$ stage of murine thymocyte development,[86] were detected in thymocytes[53] and peripheral T cells[55] from CD3ζ-deficient mice. These data demonstrated that lack of CD3ζ expression resulted in a severe, but incomplete, block in thymocyte development at the $CD4^+CD8^+$ stage in these animals. Thymocytes were not available for analysis from the SCID infant described in this report. However, TCRβ gene rearrangements were detected in the periphery (Figure 2) and the phenotype of circulating patient $CD3\varepsilon^{low}$ cells (Table 1; Figures 1 and 4) was nearly identical to that noted in $CD3\zeta^{-/-}$ mice.[52-55] These findings suggest the defects in T-cell development caused by complete CD3ζ deficiency in mice and humans are similar. CD3ζ plays an important role in TCR-mediated signaling via its 3 ITAMs and is also required for assembly and efficient surface expression of the multimeric TCR complex. The observation that T-cell development was restored in CD3ζ-deficient animals by transgenic CD3ζ chains lacking signal transducing ITAMs[87] suggested the ability of CD3ζ to promote TCR surface expression was critical for murine thymocyte development but that CD3ζ ITAM signaling was not required for this process. A subsequent analysis of signaling-defective CDζ transgenic $CD3\zeta^{-/-}$ mice expressing the H-Y TCR transgene did suggest a role for CD3ζ signaling in amplifying TCR signals during thymocyte positive and negative selection.[88] The deranged TCR assembly and surface expression noted in patient T cells and MA5.8 cells transduced with patient mutant CD3ζ in the present report suggests the role CD3ζ plays in TCR assembly and expression is also essential for normal human T-cell development.

The homozygous 411insC CD3ζ gene mutation noted in our SCID infant led to complete CD3ζ deficiency with no protein detected in patient $CD3\varepsilon^{low}$ cells or retrovirally transduced MA5.8 cells. D138fsX272 chains encoded by 411insC mutant patient CD3ζ alleles are predicted to lack the final 26 residues of wild-type protein that include the third intracellular ITAM, and instead contain 134 C-terminal missense amino acids that exhibit no clear-cut structure or homology with known proteins and lack identifiable sequence motifs. Neither homology searches nor molecular modeling analysis have provided clear insight into how the C-terminal missense extension might prevent stable CD3ζ expression and incorporation into patient TCR complexes. Our

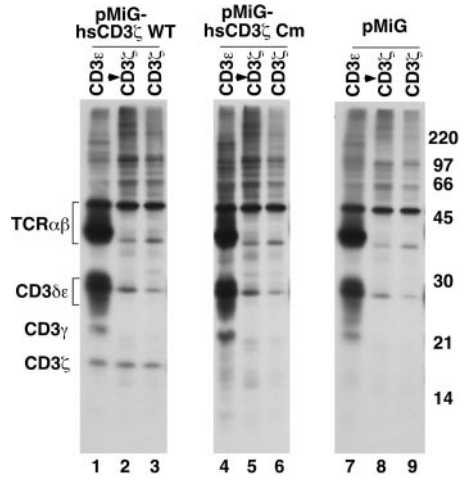

Figure 7. MA5.8 cells transduced with patient mutant CD3ζ cDNA do not express detectable CD3ζ protein and fail to assemble complete TCR complexes. MA5.8 hybridoma cells retrovirally transduced with the indicated human CD3ζ cDNAs or pMiG vector alone were metabolically labeled for 30 minutes and lysed in digitonin lysis buffer. Lysates were either sequentially immunoprecipitated with anti-CD3ε Ab followed by anti-CD3ζ Ab or immunoprecipitated with anti-CD3ζ Ab alone. Immunoprecipitated material was resolved by SDS-PAGE and TCR chains visualized by fluorography.

inability to identify nascent D138fsX272 mutant protein in metabolically labeled, transduced MA5.8 cells indicated the elongated mutant CD3ζ chains were unstable and rapidly degraded. This finding was unlikely to be simply due to poor expression of mutant CD3ζ cDNA by the pMiG vector in these experiments because (1) endogenous mutant CD3ζ protein was also undetectable in patient CD3ε^{low} cells, despite normal steady-state levels of CD3ζ mRNA (Figure 4), (2) wild-type and patient mutant CD3ζ cDNAs only differ by one coding region nucleotide, and (3) the observed comparable expression of GFP protein in MA5.8 cells transduced with wild-type or mutant CD3ζ constructs (Figure 6A) demonstrated that the common bicistronic transcriptional unit of the vector[75] encoding both GFP and CD3ζ insert was efficiently expressed in these cells.

The findings in the present study examining complete CD3ζ deficiency also extend those of a recent report describing a patient with recurrent infections and decreased numbers of peripheral T cells due to a complex, partial deficiency of CD3ζ protein expression.[60] In that report, 90% of the patient's T cells exhibited low surface TCRαβ and CD3ε expression, and very low levels of CD3ζ protein, which was only detectable in the cytoplasm. The remaining 10% of patient-origin T cells displayed normal surface TCRαβ, CD3ε, and CD3ζ expression but lacked detectable anti-CD3ε–mediated ZAP-70 phosphorylation.[60] Patient T cells with low TCR expression were homozygous for a germline Q70X CD3ζ mutation, whereas cells with normal TCR expression exhibited partial correction of the germline Q70X present on one allele by one of 3 different missense somatic mutations of Q70X found on the other allele.[60] An increased frequency of CD4$^-$CD8$^-$CD3ε$^+$ cells was not noted in the patient with CD3ζ deficiency partially corrected by somatic mutations, presumably because partial correction of the CD3ζ mutation returned surface TCR expression to a more normal level. Differences in NK cell development and function were also apparent between the described patient with partial CD3ζ deficiency[60] and the SCID infant due to complete CD3ζ deficiency reported herein. This finding is of interest because CD3ζ subunits have been shown to associate with CD16,[89,90] NKp46,[91] and NKp30[92] NK receptors and transduce activation signals. Normal numbers of CD56$^+$CD16$^+$ NK cells that exhibited normal cytotoxicity of K562 targets were noted in the reported human case of partially corrected CD3ζ deficiency.[60] CD3ζ$^{-/-}$ mice also exhibited normal NK activity against YAC-1 target cells, demonstrating CD3ζ was not essential for murine NK cell development and function.[55] However, in the present report, normal numbers of CD16$^+$ cells were present but the NK cells lacked detectable coexpression of CD56 on the cell surface (Table 1) and exhibited diminished lytic activity against K562 targets at all E/T ratios tested (Figure 3). The CD56$^-$CD16$^+$ cells present in our patient possibly represent the previously described dysfunctional and rare CD56$^-$CD16$^+$ subset of human NK cells that is greatly expanded in HIV-viremic patients.[93-95] CD56$^-$CD16$^+$ NK cells exhibit altered expression of certain inhibitory and activating NK receptors and poor lytic activity against K562 targets.[95] Although we have not noted CD56$^-$CD16$^+$ cells in other patients with CMV infection and are not aware of any reports describing a role for this NK subset in the response to CMV, it is conceivable this virus may have been responsible for expansion of CD56$^-$CD16$^+$ NK cells in our patient. Alternatively, CD56$^-$CD16$^+$ cells may be the only NK subset that develops in the setting of complete human CD3ζ deficiency. Studies to further characterize the NK cells in our patient are planned. CD56$^-$CD16$^+$ cells were not noted in the child with partially corrected CD3ζ deficiency reported previously.[60] However, that patient exhibited 2 distinct populations of T cells, in terms of CD3ζ expression, and may have likewise expressed more than one population of NK cells.

In conclusion, the present study describes a case of T$^-$B$^+$NK$^+$ SCID due to a homozygous 411insC mutation in the CD3ζ gene that, to our knowledge, is the first reported case of SCID attributable to complete CD3ζ deficiency. In contrast with the findings in a recent report of the first case of partial human CD3ζ deficiency,[60] the SCID patient in the present study lacked mature T cells, expressed large numbers of CD3ε^{low} CD4$^-$CD8$^-$ cells in the periphery, and exhibited an unusual population of CD56$^-$CD16$^+$ NK cells. These observations in 2 CD3ζ-deficient patients provide a second example, along with that of CD3ε deficiency,[22,57] that differences in the extent of a CD3 chain deficiency can lead to different clinical and immunologic phenotypes.

Acknowledgments

This work was supported by National Institutes of Health grants AI42951, AI47605, CA100144, CA87407, HD35961, P01CA0927, and P30-DK-50306; an appropriation from the Commonwealth of Pennsylvania; and by grant M01-RR-30 from the National Center for Research Resources, General Clinical Research Centers Program, National Institutes of Health.

The authors thank Drs Dario Vignali and David McKean for providing reagents, Drs Elizabeth Shores and Wesley Burks for reviewing the manuscript, and Dr Marian Melish for referring the patient.

Authorship

J.L.R. designed research, collected and analyzed data, and wrote the paper; J.P.H.L. designed and performed research; M.C., R.E.P., E.O.S., C.M.W., and M.D.K. performed research; J.H.C. contributed vital new reagents; J.C. performed research and analyzed data; M.S.K. contributed analytical tools and analyzed data; M.S. contributed analytical tools and analyzed data; X.-P.Z. contributed vital new reagents and analyzed data; D.L.W. contributed vital new analytical tools and reagents, designed research and analyzed data; and R.H.B. designed research and analyzed data.

Conflict-of-interest disclosure: The authors declare no competing financial interests.

Correspondence: Joseph L. Roberts, Box 2898, Duke University Medical Center, Durham, NC 27710; e-mail: rober060@mc.duke.edu.

References

1. Bortin MM, Rimm AA. Severe combined immunodeficiency disease. Characterization of the disease and results of transplantation. JAMA. 1977;238:591-600.
2. Fischer A. Severe combined immunodeficiencies (SCID). Clin Exp Immunol. 2000;122:143-149.
3. Buckley RH. Molecular defects in human severe combined immunodeficiency and approaches to immune reconstitution. Annu Rev Immunol. 2004; 22:625-655.
4. Noguchi M, Yi H, Rosenblatt HM, et al. Interleukin-2 receptor gamma chain mutation results in X-linked severe combined immunodeficiency in humans. Cell. 1993;73:147-157.
5. Puck JM, Deschenes SM, Porter JC, et al. The interleukin-2 receptor gamma chain maps to Xq13.1 and is mutated in X-linked severe combined immunodeficiency, SCIDX1. Hum Mol Genet. 1993;2:1099-1104.
6. Puel A, Ziegler SF, Buckley RH, Leonard WJ. Defective IL7R expression in T(−)B(+)NK(+) severe combined immunodeficiency. Nat Genet. 1998;20:394-397.
7. Puel A, Leonard WJ. Mutations in the gene for the

IL-7 receptor result in T(−)B(+)NK(+) severe combined immunodeficiency disease. Curr Opin Immunol. 2000;12:468-473.

8. Roifman CM, Zhang J, Chitayat D, Sharfe N. A partial deficiency of interleukin-7R alpha is sufficient to abrogate T-cell development and cause severe combined immunodeficiency. Blood. 2000;96:2803-2807.
9. Macchi P, Villa A, Giliani S, et al. Mutations of Jak-3 gene in patients with autosomal severe combined immune deficiency (SCID). Nature. 1995;377:65-68.
10. Russell SM, Tayebi N, Nakajima H, et al. Mutation of Jak3 in a patient with SCID: essential role of Jak3 in lymphoid development. Science. 1995; 270:797-800.
11. Roberts JL, Lengi A, Brown SM, et al. Janus kinase 3 (JAK3) deficiency: clinical, immunologic, and molecular analyses of 10 patients and outcomes of stem cell transplantation. Blood. 2004; 103:2009-2018.
12. Schwarz K, Gauss GH, Ludwig L, et al. RAG mutations in human B cell-negative SCID. Science. 1996;274:97-99.
13. Moshous D, Callebaut I, de Chasseval R, et al. Artemis, a novel DNA double-strand break repair/V(D)J recombination protein, is mutated in human severe combined immune deficiency. Cell. 2001; 105:177-186.
14. Li L, Moshous D, Zhou Y, et al. A founder mutation in Artemis, an SNM1-like protein, causes SCID in Athabascan-speaking Native Americans. J Immunol. 2002;168:6323-6329.
15. van der BM, van Veelen LR, Verkaik NS, et al. A new type of radiosensitive T-B-NK+ severe combined immunodeficiency caused by a LIG4 mutation. J Clin Invest. 2006;116:137-145.
16. Buck D, Moshous D, de Chasseval R, et al. Severe combined immunodeficiency and microcephaly in siblings with hypomorphic mutations in DNA ligase IV. Eur J Immunol. 2006;36:224-235.
17. Enders A, Fisch P, Schwarz K, et al. A severe form of human combined immunodeficiency due to mutations in DNA ligase IV. J Immunol. 2006; 176:5060-5068.
18. Giblett ER, Anderson JE, Cohen F, Pollara B, Meuwissen HJ. Adenosine-deaminase deficiency in two patients with severely impaired cellular immunity. Lancet. 1972;2:1067-1069.
19. Kung C, Pingel JT, Heikinheimo M, et al. Mutations in the tyrosine phosphatase CD45 gene in a child with severe combined immunodeficiency disease. Nat Med. 2000;6:343-345.
20. Tchilian EZ, Wallace DL, Wells RS, et al. A deletion in the gene encoding the CD45 antigen in a patient with SCID. J Immunol. 2001;166:1308-1313.
21. Dadi HK, Simon AJ, Roifman CM. Effect of CD3delta deficiency on maturation of alpha/beta and gamma/delta T-cell lineages in severe combined immunodeficiency. N Engl J Med. 2003; 349:1821-1828.
22. de Saint BG, Geissmann F, Flori E, et al. Severe combined immunodeficiency caused by deficiency in either the delta or the epsilon subunit of CD3. J Clin Invest. 2004;114:1512-1517.
23. Klausner RD, Lippincott-Schwartz J, Bonifacino JS. The T cell antigen receptor: insights into organelle biology. Annu Rev Cell Biol. 1990;6:403-431.
24. Strominger JL. Developmental biology of T cell receptors. Science. 1989;244:943-950.
25. Bluestone JA, Cron RQ, Rellahan B, Matis LA. Ligand specificity and repertoire development of murine TCR gamma delta cells. Curr Top Microbiol Immunol. 1991;173:133-139.
26. Moretta L, Ciccone E, Ferrini S, et al. Molecular and cellular analysis of human T lymphocytes expressing gamma delta T-cell receptor. Immunol Rev. 1991;120:117-135.
27. Ohashi PS, Mak TW, Van den EP, et al. Reconstitution of an active surface T3/T-cell antigen receptor by DNA transfer. Nature. 1985;316:606-609.
28. Saito T, Weiss A, Gunter KC, Shevach EM, Germain RN. Cell surface T3 expression requires the presence of both alpha- and beta-chains of the T cell receptor. J Immunol. 1987;139:625-628.
29. Alarcon B, Berkhout B, Breitmeyer J, Terhorst C. Assembly of the human T cell receptor-CD3 complex takes place in the endoplasmic reticulum and involves intermediary complexes between the CD3-gamma.delta.epsilon core and single T cell receptor alpha or beta chains. J Biol Chem. 1988;263:2953-2961.
30. Bonifacino JS, Lippincott-Schwartz J, Chen C, et al. Association and dissociation of the murine T cell receptor associated protein (TRAP). Early events in the biosynthesis of a multisubunit receptor. J Biol Chem. 1988;263:8965-8971.
31. Geisler C, Kuhlmann J, Rubin B. Assembly, intracellular processing, and expression at the cell surface of the human alpha beta T cell receptor/CD3 complex. Function of the CD3-zeta chain. J Immunol. 1989;143:4069-4077.
32. Sancho J, Chatila T, Wong RC, et al. T-cell antigen receptor (TCR)-alpha/beta heterodimer formation is a prerequisite for association of CD3-zeta 2 into functionally competent TCR.CD3 complexes. J Biol Chem. 1989;264:20760-20769.
33. Dietrich J, Kastrup J, Lauritsen JP, et al. TCRzeta is transported to and retained in the Golgi apparatus independently of other TCR chains: implications for TCR assembly. Eur J Immunol. 1999;29: 1719-1728.
34. Sussman JJ, Bonifacino JS, Lippincott-Schwartz J, et al. Failure to synthesize the T cell CD3-zeta chain: structure and function of a partial T cell receptor complex. Cell. 1988;52:85-95.
35. Hall C, Berkhout B, Alarcon B, et al. Requirements for cell surface expression of the human TCR/CD3 complex in non-T cells. Int Immunol. 1991;3:359-368.
36. Davis MM, Bjorkman PJ. T-cell antigen receptor genes and T-cell recognition. Nature. 1988;334: 395-402.
37. Reth M. Antigen receptor tail clue. Nature. 1989; 338:383-384.
38. Samelson LE, Klausner RD. Tyrosine kinases and tyrosine-based activation motifs. Current research on activation via the T cell antigen receptor. J Biol Chem. 1992;267:24913-24916.
39. Romeo C, Amiot M, Seed B. Sequence requirements for induction of cytolysis by the T cell antigen/Fc receptor zeta chain. Cell. 1992;68:889-897.
40. Irving BA, Chan AC, Weiss A. Functional characterization of a signal transducing motif present in the T cell antigen receptor zeta chain. J Exp Med. 1993;177:1093-1103.
41. Chan AC, Iwashima M, Turck CW, Weiss A. ZAP-70: a 70 kd protein-tyrosine kinase that associates with the TCR zeta chain. Cell. 1992;71:649-662.
42. Kong G, Dalton M, Wardenburg JB, et al. Distinct tyrosine phosphorylation sites in ZAP-70 mediate activation and negative regulation of antigen receptor function. Mol Cell Biol. 1996;16:5026-5035.
43. Fehling HJ, Krotkova A, Saint-Ruf C, von Boehmer H. Crucial role of the pre-T-cell receptor alpha gene in development of alpha beta but not gamma delta T cells. Nature. 1995;375:795-798.
44. von Boehmer H. Control of T-cell development by the pre-T and alpha beta T-cell receptor. Ann N Y Acad Sci. 1995;766:52-61.
45. Robey E, Fowlkes BJ. Selective events in T cell development. Annu Rev Immunol. 1994;12:675-705.
46. Jameson SC, Hogquist KA, Bevan MJ. Positive selection of thymocytes. Annu Rev Immunol. 1995;13:93-126.
47. Mombaerts P, Clarke AR, Rudnicki MA, et al. Mutations in T-cell antigen receptor genes alpha and beta block thymocyte development at different stages. Nature. 1992;360:225-231.
48. Haks MC, Krimpenfort P, Borst J, Kruisbeek AM. The CD3gamma chain is essential for development of both the TCRalphabeta and TCRgammadelta lineages. EMBO J. 1998;17:1871-1882.
49. Malissen M, Gillet A, Ardouin L, et al. Altered T cell development in mice with a targeted mutation of the CD3-epsilon gene. EMBO J. 1995;14: 4641-4653.
50. Philpott KL, Viney JL, Kay G, et al. Lymphoid development in mice congenitally lacking T cell receptor alpha beta-expressing cells. Science. 1992;256:1448-1452.
51. Dave VP, Cao Z, Browne C, et al. CD3 delta deficiency arrests development of the alpha beta but not the gamma delta T cell lineage. EMBO J. 1997;16:1360-1370.
52. Love PE, Shores EW, Johnson MD, et al. T cell development in mice that lack the zeta chain of the T cell antigen receptor complex. Science. 1993;261:918-921.
53. Malissen M, Gillet A, Rocha B, et al. T cell development in mice lacking the CD3-zeta/eta gene. EMBO J. 1993;12:4347-4355.
54. Ohno H, Aoe T, Taki S, et al. Developmental and functional impairment of T cells in mice lacking CD3 zeta chains. EMBO J. 1993;12:4357-4366.
55. Liu CP, Ueda R, She J, et al. Abnormal T cell development in CD3-zeta$^{-/-}$ mutant mice and identification of a novel T cell population in the intestine. EMBO J. 1993;12:4863-4875.
56. Le Deist F, Thoenes G, Corado J, Lisowska-Grospierre B, Fischer A. Immunodeficiency with low expression of the T cell receptor/CD3 complex. Effect on T lymphocyte activation. Eur J Immunol. 1991;21:1641-1647.
57. Soudais C, de Villartay JP, Le Deist F, Fischer A, Lisowska-Grospierre B. Independent mutations of the human CD3-epsilon gene resulting in a T cell receptor/CD3 complex immunodeficiency. Nat Genet. 1993;3:77-81.
58. Arnaiz-Villena A, Timon M, Corell A, et al. Brief report: primary immunodeficiency caused by mutations in the gene encoding the CD3-gamma subunit of the T-lymphocyte receptor. N Engl J Med. 1992;327:529-533.
59. Perez-Aciego P, Alarcon B, Arnaiz-Villena A, et al. Expression and function of a variant T cell receptor complex lacking CD3-gamma. J Exp Med. 1991;174:319-326.
60. Rieux-Laucat F, Hivroz C, Lim A, et al. Inherited and somatic CD3zeta mutations in a patient with T-cell deficiency. N Engl J Med. 2006;354:1913-1921.
61. Pannetier C, Even J, Kourilsky P. T-cell repertoire diversity and clonal expansions in normal and clinical samples. Immunol Today. 1995;16:176-181.
62. Douek DC, Vescio RA, Betts MR, et al. Assessment of thymic output in adults after haematopoietic stem-cell transplantation and prediction of T-cell reconstitution. Lancet. 2000;355:1875-1881.
63. Sarzotti M, Patel DD, Li X, et al. T cell repertoire development in humans with SCID after nonablative allogeneic marrow transplantation. J Immunol. 2003;170:2711-2718.
64. Kepler TB, He M, Tomfohr JK, et al. Statistical analysis of antigen receptor spectratype data. Bioinformatics. 2005;21:3394-3400.
65. Buckley RH, Schiff SE, Sampson HA, et al. Development of immunity in human severe primary T cell deficiency following haploidentical bone marrow stem cell transplantation. J Immunol. 1986;136:2398-2407.
66. Weissman AM, Samelson LE, Klausner RD. A new subunit of the human T-cell antigen receptor complex. Nature. 1986;324:480-482.
67. Altschul SF, Madden TL, Schaffer AA, et al.

Gapped BLAST and PSI-BLAST: a new generation of protein database search programs. Nucleic Acids Res. 1997;25:3389-3402.

68. Jones DT. Protein secondary structure prediction based on position-specific scoring matrices. J Mol Biol. 1999;292:195-202.
69. Canutescu AA, Dunbrack RL Jr. MolIDE: a homology modeling framework you can click with. Bioinformatics. 2005;21:2914-2916.
70. Berman HM, Westbrook J, Feng Z, et al. The Protein Data Bank. Nucleic Acids Res. 2000;28:235-242.
71. Krogh A, Larsson B, von Heijne G, Sonnhammer EL. Predicting transmembrane protein topology with a hidden Markov model: application to complete genomes. J Mol Biol. 2001;305:567-580.
72. Moingeon P, Stebbins CC, D'Adamio L, Lucich J, Reinherz EL. Human natural killer cells and mature T lymphocytes express identical CD3 zeta subunits as defined by cDNA cloning and sequence analysis. Eur J Immunol. 1990;20:1741-1745.
73. Wu J, Edberg JC, Gibson AW, Tsao B, Kimberly RP. Single-nucleotide polymorphisms of T cell receptor zeta chain in patients with systemic lupus erythematosus. Arthritis Rheum. 1999;42:2601-2605.
74. Atkinson TP, Hall CG, Goldsmith J, Kirkham PM. Splice variant in TCRzeta links T cell receptor signaling to a G-protein-related signaling pathway. Biochem Biophys Res Commun. 2003;310:761-766.
75. Liu X, Sun Y, Constantinescu SN, et al. Transforming growth factor beta-induced phosphorylation of Smad3 is required for growth inhibition and transcriptional induction in epithelial cells. Proc Natl Acad Sci U S A. 1997;94:10669-10674.
76. Pear WS, Miller JP, Xu L, et al. Efficient and rapid induction of a chronic myelogenous leukemia-like myeloproliferative disease in mice receiving P210 bcr/abl-transduced bone marrow. Blood. 1998;92:3780-3792.
77. Haks MC, Belkowski SM, Ciofani M, et al. Low activation threshold as a mechanism for ligand-independent signaling in pre-T cells. J Immunol. 2003;170:2853-2861.
78. Carleton M, Haks MC, Smeele SA, et al. Early growth response transcription factors are required for development of CD4(−)CD8(−) thymocytes to the CD4(+)CD8(+) stage. J Immunol. 2002;168:1649-1658.
79. Kubo RT, Born W, Kappler JW, Marrack P, Pigeon M. Characterization of a monoclonal antibody which detects all murine alpha beta T cell receptors. J Immunol. 1989;142:2736-2742.
80. Leo O, Foo M, Sachs DH, Samelson LE, Bluestone JA. Identification of a monoclonal antibody specific for a murine T3 polypeptide. Proc Natl Acad Sci U S A. 1987;84:1374-1378.
81. Kearse KP, Roberts JL, Munitz TI, et al. Developmental regulation of alpha beta T cell antigen receptor expression results from differential stability of nascent TCR alpha proteins within the endoplasmic reticulum of immature and mature T cells. EMBO J. 1994;13:4504-4514.
82. Wiest DL, Burgess WH, McKean D, Kearse KP, Singer A. The molecular chaperone calnexin is expressed on the surface of immature thymocytes in association with clonotype-independent CD3 complexes. EMBO J. 1995;14:3425-3433.
83. Carleton M, Ruetsch NR, Berger MA, et al. Signals transduced by CD3epsilon, but not by surface pre-TCR complexes, are able to induce maturation of an early thymic lymphoma in vitro. J Immunol. 1999;163:2576-2585.
84. Schreiber KL, Bell MP, Huntoon CJ, et al. Class II histocompatibility molecules associate with calnexin during assembly in the endoplasmic reticulum. Int Immunol. 1994;6:101-111.
85. Lauritsen JP, Bonefeld CM, von Essen M, et al. Masking of the CD3 gamma di-leucine-based motif by zeta is required for efficient T-cell receptor expression. Traffic. 2004;5:672-684.
86. Godfrey DI, Kennedy J, Mombaerts P, Tonegawa S, Zlotnik A. Onset of TCR-beta gene rearrangement and role of TCR-beta expression during $CD3^{-}CD4^{-}CD8^{-}$ thymocyte differentiation. J Immunol. 1994;152:4783-4792.
87. Shores EW, Huang K, Tran T, et al. Role of TCR zeta chain in T cell development and selection. Science. 1994;266:1047-1050.
88. Shores EW, Tran T, Grinberg A, et al. Role of the multiple T cell receptor (TCR)-zeta chain signaling motifs in selection of the T cell repertoire. J Exp Med. 1997;185:893-900.
89. Anderson P, Caligiuri M, O'Brien C, et al. Fc gamma receptor type III (CD16) is included in the zeta NK receptor complex expressed by human natural killer cells. Proc Natl Acad Sci U S A. 1990;87:2274-2278.
90. Lanier LL, Yu G, Phillips JH. Co-association of CD3 zeta with a receptor (CD16) for IgG Fc on human natural killer cells. Nature. 1989;342:803-805.
91. Vitale M, Bottino C, Sivori S, et al. NKp44, a novel triggering surface molecule specifically expressed by activated natural killer cells, is involved in non-major histocompatibility complex-restricted tumor cell lysis. J Exp Med. 1998;187:2065-2072.
92. Pende D, Parolini S, Pessino A, et al. Identification and molecular characterization of NKp30, a novel triggering receptor involved in natural cytotoxicity mediated by human natural killer cells. J Exp Med. 1999;190:1505-1516.
93. Scott-Algara D, Paul P. NK cells and HIV infection: lessons from other viruses. Curr Mol Med. 2002;2:757-768.
94. Mavilio D, Benjamin J, Daucher M, et al. Natural killer cells in HIV-1 infection: dichotomous effects of viremia on inhibitory and activating receptors and their functional correlates. Proc Natl Acad Sci U S A. 2003;100:15011-15016.
95. Mavilio D, Lombardo G, Benjamin J, et al. Characterization of $CD56^{-}/CD16^{+}$ natural killer (NK) cells: a highly dysfunctional NK subset expanded in HIV-infected viremic individuals. Proc Natl Acad Sci U S A. 2005;102:2886-2891.